Enhanced Multi-Channel Active Fuzzy Neural Network Noise Control in an Enclosure

Navid Azadi, Abdolreza Ohadi

***Abstract*—The performance of conventional linear algorithms in Active Noise Control (ANC) applications deteriorates facing nonlinearities in the system, which is mainly due to loudspeakers. On the other hand, fuzzy logic and neural networks are good candidates to overcome this drawback. In this paper the acoustic attenuation of noise in a rectangular enclosure with a flexible panel and 5 rigid walls is presented using a multi-channel enhanced fuzzy neural network (EFNN) error back propagation algorithm while taking into account the secondary path effect in derivation of equations. The phrase *enhanced* represents the secondary path effect in derivation of EFNN controller. The primary path in the system comprises a nonlinear model of loudspeaker, parameters of which vary with the input current. Next, the performance of FXLMS and enhanced fuzzy neural network algorithms are compared and it is observed that fuzzy neural network controller exhibits better results in the presence of loudspeakers with nonlinear behavior.**

***Index Terms*—Active Noise Control, Fuzzy Neural Networks, Nonlinear Loudspeaker, FXLMS, 3D Enclosure, Flexible Panel.**

I. Introduction

IN integration with Passive Noise Control techniques, an Active Noise Control system can introduce a more efficient noise cancellation in systems. These systems are widely incorporated in air conditioning systems as well as vehicles and public transportation systems. Active Noise Control systems are based on the principle of superposition of waves, in which the noise sound wave is canceled with anti-noise sound wave as illustrated in Fig. 1 . Anti-noise wave should specifically have the same amplitude as noise, but should be in 180 of phase shift. This task is done using an adaptively tuned algorithm in the secondary path of the ANC system.

In most of applications of ANC systems, a linear algorithm is used to generate the anti-noise signal. A vivid example is the FXLMS algorithm, in which an FIR filter is employed in such a way for the error signal to be minimized. On the other hand, in specific ANC systems primary path exhibits nonlinear behavior, the output signal of which a linear algorithm is not designed to cancel. In this paper, an enhanced neuro-fuzzy ANC system is implemented in a 3D enclosure with a flexible panel to minimize the noise introduced in the system by an internal nonlinear noise source, namely, a nonlinear loudspeaker.

Kim and Brenna in [1], [2], [3] discussed the acoustic-structure couple in a rectangular enclosure with a simply supported flexible panel in 1999. They also studied the propagation of a plane wave into the enclosure through the flexible panel. Later in 2003, Jorge introduced an analytical model for the vibration of rectangular clamped plate using virtual work principle and verified his results with finite element method [4]. In addition, in 2007, Wu et al. presented an exact solution for free vibration analysis of rectangular plate using Bessel functions. The formulations introduced here in this article are derived using these two references [5].

Regarding the modeling of nonlinear loudspeaker, Ravaud [6] presented a timevarying nonlinear model of an electro-dynamic loudspeaker. In this article, two coupled differential equations, one for displacement of diaphragm and the other for magnetic field in the loudspeaker, are introduced and then based on these two equations, a nonlinear model in presented. There is lots of information available in the field of linear Active Noise Control in text books. LMS algorithm and its derivatives like FXLMS and NLMS are widely discussed in [7] . On the other hand, nonlinear ANC is a rather new field of study. In 2000, Carmona et al. [8] implemented an active noise control in a duct using pole placement and sensitivity function reshaping in robust control. Recently, Neural Networks and Fuzzy control are also implicated in ANC application. In 2002, active noise hybrid feedforward/feedback control using neural network compensation was performed, in which error gradient descent is employed to update neural network parameters [9]. Later in 2004, a simplified Fuzzy-Neral Network control algorithm was introduced [11] and was improved in 2006 by the same author as Adaptive Recurrent Fuzzy Neural Network for Active Noise Control. Furthermore, this controller was implemented on the acoustic field in a duct in 2008. The effect of secondary path was not studied in none of these algorithms. As an amendment, Rastegar and Ohadi in 2009 examined the implementation of secondary path in derivation of equations [12]. They showed the effect of secondary path by carrying out simulations on the acoustic field in an enclosure with a flexible panel.

In this article the effect of introduction of secondary path transfer function in derivation of a fuzzy-neural network

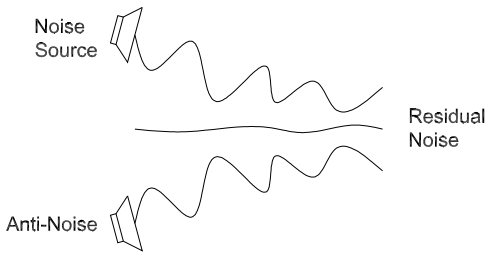

Fig. 1. Schematic illustration of the principle of superposition of waves.

Manuscript received March 05, 2011; revised March 29, 2011.

AbdolReza Ohadi is an associate professor at the Department of Mechanical Engineering, AmirKabir University of Technology, Tehran, Iran, e-mail: a_r_ohadi@aut.ac.ir.

Navid Azadi is an MSc graduate at AmirKabir University of Technology, Tehran, Iran, e-mail: navid.azadi@gmail.com.

ISBN: 978-988-19251-5-2
ISSN: 2078-0958 (Print); ISSN: 2078-0966 (Online)

controller for the attenuation of acoustic noise in a cubic enclosure with 5 rigid walls and a flexible clamped plate is investigated in simulations.

II. Modeling of Enclosure with Flexible Panel

In this section, modeling of acoustic-structure couple in the enclosure is briefly studied. All the variables used in this section are defined in Table I. As shown in Fig. 2 and accroding to [1], the governing partial differential equation of vibration of a rectangular plate is like (1).

$$D_p \nabla^4 w\left(y_1, y_2, t\right) + \rho_p h_p \frac{\partial^2 w\left(y_1, y_2, t\right)}{\partial t^2} = F_p\left(y_1, y_2, t\right), \quad (1)$$

Boundary limits and boundary conditions for a clamped rectangular plate are defined as (2) and (3), respectively.

$$0 \leq y_1 \leq L_2\,, \;\; 0 \leq y_2 \leq L_3 \quad (2)$$

$$w = 0, \quad {}^{\partial w}/_{\partial n} = 0 \quad (3)$$

On the other hand, the acoustic enclosure is modeled via a partial differential equation as described by (4), which is derived using laws of *continuity of mass* and *continuity of momentum*.

$$\begin{aligned} &\nabla^2 P\left(t, \mathbf{x}\right) - \frac{1}{c_0^2} \frac{\partial^2 P\left(t, \mathbf{x}\right)}{\partial t^2} = \\ &-\rho_0 \frac{\partial^2 W\left(x_2, x_3, t\right)}{\partial t^2} \delta\left(x_1 - L_1\right) - \rho_0 \dot{u}_{sp}\left(t\right) Pos_{sp}\left(\mathbf{x}_{sp}\right), \end{aligned} \quad (4)$$

Boundary conditions for the enclosure are defined so that there is no gradient of pressure on the walls, mathematical interpretation of this statement is like (5).

$$\nabla P\left(t, \mathbf{x}\right).n = 0 \quad on \quad \Omega_B \quad (5)$$

Manipulating equations (1) and (4), two coupled differential equations describing this coupled vibro-acoustic problem are derived in (6) and (7).

$$\begin{aligned} &\ddot{q}_n\left(t\right) + 2\xi_{a,n}\omega_{a,n}\dot{q}_n\left(t\right) + \omega_{a,n}^2 q_n\left(t\right) = \\ &\frac{c_0^2 \rho_0}{V_a}\left[\sum_{m=1}^{N_p} c_{n,m}\ddot{\eta}_m\left(t\right) + g_{SP,n}\left(t\right)\right] \end{aligned} \quad (6)$$

$$\begin{aligned} &\ddot{\eta}_m\left(t\right) + \omega_{p,m}^2 \eta_m\left(t\right) = \frac{1}{m_p} \\ &\int_{S_p}\int \phi_m\left(y_1, y_2\right) p_{in}\left(y_1, y_2, t\right) dy_1 dy_2, \end{aligned} \quad (7)$$

Defining state space variables like

$$\left\{ \begin{array}{c} x_m^p \\ y_m^p \end{array} \right\} = \left\{ \begin{array}{c} \eta_m\left(t\right) \\ \dot{\eta}_m\left(t\right) \end{array} \right\}, \left\{ \begin{array}{c} x_n^a \\ y_n^a \end{array} \right\} = \left\{ \begin{array}{c} q_n\left(t\right) \\ \dot{q}_n\left(t\right) \end{array} \right\} \quad (8)$$

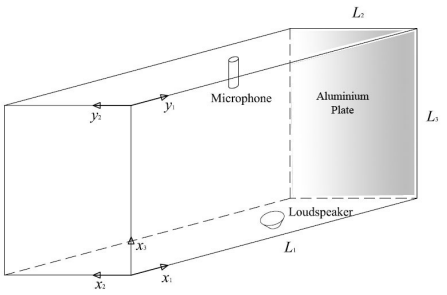

Fig. 2. Cubic coupled acoustic-structure enclosure with 5 rigid walls and a flexible panel including coordinate systems.

the state space model of the whole system is derived as (9).

$$\dot{\mathbf{X}}_{state} = \mathbf{A}_{state}^{new}\mathbf{X}_{state} + \mathbf{D}_{SP}^{new}\mathbf{f}_{SP} \quad (9)$$

in which, $\mathbf{f}_{SP}$ is the excitation of this state space model and in related to pressure exerted in the enclosure by a loudspeaker. In this equation states are define in (10).

$$\mathbf{x}_{state} = \left\{ \begin{array}{cccccccc} \{ & x_1^p & y_1^p & x_2^p & y_2^p & \dots & x_m^p & y_m^p & \}^T \\ \{ & x_0^a & y_0^a & x_1^a & y_1^a & \dots & x_n^a & y_n^a & \}^T \end{array} \right\} \quad (10)$$

The model of the enclosure, from pressure in one point to pressure in another, is now at hand. In the next step, using a nonlinear model of loudspeaker as what defined in [6], transfer function between input voltage of a loudspeaker inside the enclosure and the pressure in another point would be at hand. In the next section, a controller is designed to attenuate pressure fluctuations (or noise) induced in the enclosure by this loudspeaker using a linear loudspeaker.

III. Structure of ANC System

Schematic diagram of an active fuzzy neural network active noise control system is shown in Fig. 3 . Error signal is described as (11).

$$e\left(n\right) = d\left(n\right) - S\left(z\right) y^{(5)}\left(n\right) \quad (11)$$

where $e\left(n\right)$ is error signal, $d\left(n\right)$ is desired signal generated by nonlinear primary path, $P\left(z\right)$, and $y^{(5)}$ is control signal at step n handed in to $S\left(z\right)$, the transfer function of secondary path. The z-transform of (11) is presented as (12).

$$E\left(z\right) = P\left(z\right) X\left(z\right) - S\left(z\right) Y^{(5)}\left(z\right) \quad (12)$$

In practical ANC applications, $S\left(z\right)$ is unknown and must be estimated by an additional filter, $\hat{S}\left(z\right)$. Therefore, (12) is modified to (13).

TABLE I
Nomenclature in Enclosure Modeling.

Symbol	Description
(x_1, x_2, x_3)	Coordinates of enclosure
(y_1, y_2)	Coordinates of plate
(L_1, L_2, L_3)	Dimentions of enclosure
c_0	Speed of sound
$c_{n,m}$	Coupling coefficient
D_p	Flexural rigidity of plate
E_p	Young's modulus of elasticity
$g_{sp,n}$	Modal pressure of loudspeakers on enclosure
h_p	Flexible panel thickness
m_p	Mass of plate
P	Pressure inside the enclosure
p_{in}	Dynamic pressure inside the enclosure
$Pos_{sp,l}$	Position of loudspeaker
$q_n\left(t\right)$	Modal coordinates of air
V_a	Volume of enclosure
w	Lateral vibration of plate
$\eta_m\left(t\right)$	Modal coordinates of plate
Ω_B	Boundary of enclosure
ω_a	Natural frequency of air
ω_p	Natural frequency of plate
ϕ_m	Modal function of vibration of plate
ρ_p	Destity of plate
ν_p	Poisson's ratio of plate
ρ_a	Destity of air
ξ_a	Damping coefficient of air

ISBN: 978-988-19251-5-2
ISSN: 2078-0958 (Print); ISSN: 2078-0966 (Online)

$$E(z) = P(z)X(z) - \hat{S}(z)Y^{(5)}(z) \tag{13}$$

Assuming $\hat{S}(z)$ to be a vector of length l_f of weights $b_i, i = 1, 2, ...l_f$, equation (11) can be presented as (14).

$$e(n) = d(n) - \left[b_1 y^{(5)}(n) + b_2 y^{(5)}(n-1) + ... + b_{l_f} y^{(5)}(n-l_f)\right] \tag{14}$$

Hence, the cost function can be introduced in (15).

$$E(n) = \frac{1}{2}\left[d(n) - \left(b_1 y^{(5)}(n) + ... + b_{l_f} y^{(5)}\left(n-l_f\right)\right)\right]^2 \tag{15}$$

Existence of $\hat{S}(z)$ in (15) insinuates that secondary path effect has to be acconted for in derivation of governing equations of controller. Consequently, $E(n)$ is to be minimized using *steepest gradient* method in order for $e(n)$ to approach zero.

IV. Introduction to Enhanced Fuzzy Neural Network ANC

In this section, an enhanced fuzzy neural network active noise control system is presented in single channel mode using [11], [12] and then it is developed to multi-channel case. It is worth mentioning that the word "Enhanced" implies that in derivation of controller equations, the secondary path effect in behavoir of system is taken into consideration.

A. Single Channel FNN Structure

The structure of a fuzzy neural network controller is illustrated in Fig. 4. As shown in this figure, this control algorithm comprises 5 layers. namely, input layer, fuzzification layer, rule base layer, inference layer and defuzzification layer. Inference system implimented in this controller is of Mamdani-type. In layer 1, each crisp signal, x_i is transmitted to the next layer in each node.

$$y_i^{(1)} = x_i, \quad i = 0, 1, ..., m \tag{16}$$

Fuzzification is carried out in layer 2 using a Gaussian activation function.

$$y_{ij}^{(2)} = \exp\left(-\left(\frac{y_j^{(1)} - c_{ij}}{\sigma_{ij}}\right)^2\right), \quad j = 0, 1, ..., n. \tag{17}$$

in which c_{ij} and σ_{ij} are center and width of this membership function, respectively. Reasoning in fuzzy logic is performed using t-norm or min in layer 3. This is done considering fuzzy logic product introduced in (18).

$$y_j^{(3)} = C_j = \prod_{i=1}^{m} y_{ij}^{(2)} \tag{18}$$

Mamdani inference is what carried out in layers 4 and 5 via a simple center of gravity scheme. Consequently, crisp output signal is generated in layer 5 by (21).

$$y_1^{(4)} = \sum_{j=1}^{n} y_j^{(3)} * w_j \tag{19}$$

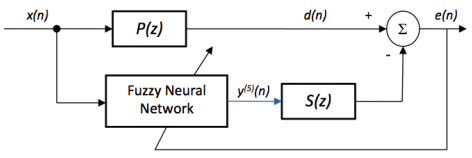

Fig. 3. Block diagram of a single channel active FNN noise control system.

$$y_2^{(4)} = \sum_{j=1}^{n} y_j^{(3)} \tag{20}$$

$$y^{(5)} = \frac{y_1^{(4)}}{y_2^{(4)}} = \frac{\sum_{j=1}^{n} y_j^{(3)} * w_j}{\sum_{j=1}^{n} y_j^{(3)}} \tag{21}$$

B. Derivation of Updating Rouls Considering the Effect of Secondary Path, Single Channel Model

In order to minimize the cost function introduced in (15), parameters like center and width of Gaussian membership function including weights of inference logic, mentioned respectively in (17) and (19), has to be tuned in each time step, n. As a result, using steepest gradient method (22), (23) and (24) are derived.

$$w_j(n+1) = w_j(n) - \eta_w \frac{\partial E(n)}{\partial w_j}, \tag{22}$$

$$c_{ij}(n+1) = c_{ij}(n) - \eta_c \frac{\partial E(n)}{\partial c_{ij}}, \tag{23}$$

$$\sigma_{ij}(n+1) = \sigma_{ij}(n) - \eta_\sigma \frac{\partial E(n)}{\partial \sigma_{ij}}. \tag{24}$$

in which η_c, η_σ and η_w are learning rate coefficients for c_{ij}, σ_{ij} and w_{ij}, respectively. Using chain roul on (15) we can have:

$$\frac{\partial E(n)}{\partial w_j} = -e(n)\left[b_1 \frac{\partial y^{(5)}(n)}{\partial w_j} + ... + b_{l_f} \frac{\partial y^{(5)}\left(n-l_f\right)}{\partial w_j}\right], \tag{25}$$

$$\frac{\partial E(n)}{\partial c_{ij}} = -e(n)\left[b_1 \frac{\partial y^{(5)}(n)}{\partial c_{ij}} + ... + b_{l_f} \frac{\partial y^{(5)}\left(n-l_f\right)}{\partial c_{ij}}\right], \tag{26}$$

$$\frac{\partial E(n)}{\partial \sigma_{ij}} = -e(n)\left[b_1 \frac{\partial y^{(5)}(n)}{\partial \sigma_{ij}} + ... + b_{l_f} \frac{\partial y^{(5)}\left(n-l_f\right)}{\partial \sigma_{ij}}\right]. \tag{27}$$

Again, applying chain rule on (21), unknown parameters in (25), (27) and (26) are derived as followings.

$$\frac{\partial y^{(5)}(n)}{\partial w_j} = \frac{\partial y^{(5)}}{\partial y_1^{(4)}} \frac{\partial y_1^{(4)}}{\partial w_j} = \left(\frac{1}{y_2^{(4)}}\right)\left(y_j^{(3)}\right), \tag{28}$$

$$\begin{aligned} \frac{\partial y^{(5)}}{\partial c_{ij}} &= \frac{\partial y^{(5)}}{\partial y_j^{(3)}} \frac{\partial y_j^{(3)}}{\partial y_{ij}^{(2)}} \frac{\partial y_{ij}^{(2)}}{\partial c_{ij}} = \\ &= \left(\frac{w_j - y^{(5)}}{y_2^{(4)}}\right).2.\left(y_j^{(3)}\right)\left(\frac{y_j^{(1)} - c_{ij}}{\sigma_{ij}^2}\right), \end{aligned} \tag{29}$$

$$\begin{aligned} \frac{\partial y^{(5)}}{\partial \sigma_{ij}} &= \frac{\partial y^{(5)}}{\partial y_j^{(3)}} \frac{\partial y_j^{(3)}}{\partial y_{ij}^{(2)}} \frac{\partial y_{ij}^{(2)}}{\partial \sigma_{ij}} = \\ &= \left(\frac{w_j - y^{(5)}}{y_2^{(4)}}\right).2.\left(y_j^{(3)}\right)\left(\frac{\left(y_j^{(1)} - c_{ij}\right)^2}{\sigma_{ij}^3}\right). \end{aligned} \tag{30}$$

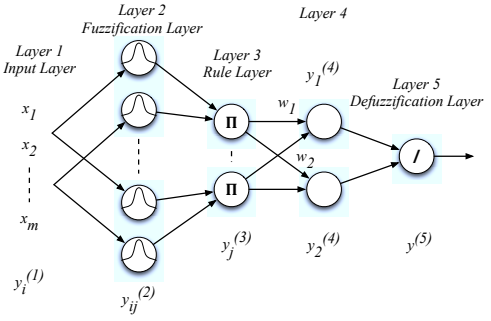

Fig. 4. Structure of back-propagation Fuzzy Neural Network control algorithm.

ISBN: 978-988-19251-5-2
ISSN: 2078-0958 (Print); ISSN: 2078-0966 (Online)

C. Derivation of Updating Rouls Considering the Effect of Secondary Path, Multi-Channel Model

In multi-channel mode, the structure of ANC system is evovled to what illustrated in Fig. 5. This is evident in Fig. 5 that in multi-channel model there are 4 secondary paths between sensors and actuators; One from error microphone no. 1 to secondary path loudspeaker 1 or $S_{11}(z)$, second, from error microphone no. 1 to secondary path loudspeaker 2 or $S_{12}(z)$, Third, from error microphone no. 2 to secondary path loudspeaker 1 or $S_{21}(z)$ and fourth, from error microphone no. 2 to secondary path loudspeaker 2 or $S_{22}(z)$. The respective identified FIR filter of these paths are $\hat{S}_{11}(z)$, $\hat{S}_{12}(z)$, $\hat{S}_{21}(z)$ and $\hat{S}_{22}(z)$.

$$E_1(z) = P(z)X(z) - Y_1^{(5)}(z)S_{11}(z) - Y_2^{(5)}(z)S_{21}(z), \quad (31)$$

$$\begin{aligned} e_1(n) &= d_1(n) - \\ &- \left[b_1 y_1^{(5)}(n) + b_2 y_1^{(5)}(n-1) + \ldots + b_{l_{f11}} y_1^{(5)}(n-l_{f11})\right] - \\ &- \left[b'_1 y_2^{(5)}(n) + b'_2 y_2^{(5)}(n-1) + \ldots + b'_{l_{f21}} y_2^{(5)}(n-l_{f21})\right], \end{aligned} \quad (32)$$

And the cost function for the first channel will be derived like (33).

$$E_1(n) = \frac{1}{2}\left\{d_1(n) - \left[b_1 y_1^{(5)}(n) + \ldots + b_{l_{f11}} y_1^{(5)}(n-l_{f11})\right] - \left[b'_1 y_2^{(5)}(n) + \ldots + b'_{l_{f21}} y_2^{(5)}(n-l_{f21})\right]\right\}^2. \quad (33)$$

Again, like what was done to derive (25), in multi-channel model using steepest gradient method correcion terms of w_j in channel 1, $\frac{\partial E_1}{\partial w_{1j}}$ and $\frac{\partial E_1}{\partial w_{2j}}$, are reproduced like (34) and (35).

$$\frac{\partial E_1}{\partial w_{1j}} = -e_1(n)\left[\frac{\partial y_1^{(5)}}{\partial w_{1j}} Filtered\ by\ \hat{S}_{11}\right], \quad (34)$$

$$\frac{\partial E_2}{\partial w_{1j}} = -e_2(n)\left[\frac{\partial y_2^{(5)}}{\partial w_{1j}} Filtered\ by\ \hat{S}_{21}\right]. \quad (35)$$

Thus, using chain rule updating equations take a form like (36) for channel 1.

$$w_{1j}(t+1) = w_{1j}(t) - \eta_{w_1}\frac{\partial E_1}{\partial w_{1j}} - \eta_{w_2}\frac{\partial E_2}{\partial w_{1j}}, \quad (36)$$

In a likesise manner as what was followed for channel 1, updating rule of w_j for channel 2 is derived like (37).

$$w_{2j}(t+1) = w_{2j}(t) - \eta_{w_1}\frac{\partial E_1}{\partial w_{2j}} - \eta_{w_2}\frac{\partial E_2}{\partial w_{2j}}. \quad (37)$$

Derivation of updating rules for c_{ij} and σ_{ij} for channel 1 and channel 2 are almost like the process followed in (36) and (37) and are not mentioned here.

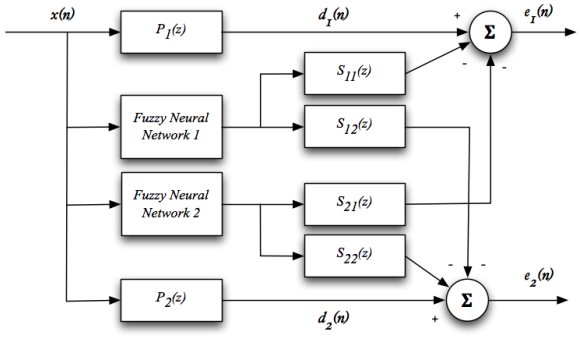

Fig. 5. Structure of multi-channel Fuzzy Neural Network control algorithm.

TABLE II
PHYSICAL PROPERTIES OF ENCLOSURE AND THE AIR INSDIE.

Symbol	Quantity	Unit	Comment
L_1	700	mm	Length of enclosure
L_2	300	mm	Width of enclosure
L_3	400	mm	Height of enclosure
h_p	5	mm	Flexible panel thickness
E_p	207×10^9	N/m^3	Young's modulus of elasticity
ρ_p	7870	Kg/m^3	Destity of plate
ν_p	0.29	-	Poisson's ratio of plate
ρ_a	1.21	Kg/m^3	Destity of air
C_0	340	m/s	Speed of sound
ξ_a	0.01	-	Damping coefficient of air

V. SIMULATION RESULTS

Simulations are performed in an enclosure with 5 rigid walls and an aluminum plate as a flexible wall. The physical properties of this enclosure including their quantity are listed in Table II. In order to generate a noise, a nonlinear loudspeaker is integrated in the enclosure. In addition, two linear loudspeakers are implemented to control the inside noise of the enclosure at the position of two error microphones. Coordinates of these elements are provided in Table III. Results of ANC in the system using Enhanced FNN controller developed here are compared with those of FXLMS algorithm in Fig. IV and Fig. 7. Simulations are performed in two cases; First, a linear case, with an input of 420 Hz sine signal and second, a nonlinear case, in which a 90 Hz sine signal is introduced to the noise loudspeaker. This is evident in Fig. 7 that nonlinear response of the loudspeaker is revealed in residual harmonics of the excitation frequency, *il. et.*, excited frequencies of 180 Hz, 270 Hz in Fig. 7 (b) and (c). The amounts of sound attenuation in the enclosure in dB in these two frequencies including their nonlinear harmonics are given in Tables IV & V. This is evident that in presence of highly nonlinear behavior of primary path, Enhaced FNN algorithm outperformes FXLMS. This is because of the nonlinear nature of FNN controller.

VI. CONCLUSION

In this paper fuzzy neural network is implemented as an algorithm to attenuate acoustic noise in an enclosure with 5 rigid walls and a flexible panel. In the derivation of the updating rules, the effect of secondary path is included and the resulting system is developed to multi-channel case. The results show that Enhanced FNN algorithm outperformes FXLMS algorithm when there is a highly nonlinear primary path in the ANC system.

TABLE III
SENSOR AND ACTUATOR POSITIONS IN THE ANC SYSTEM.

No.	Item	Position (mm)
1	Noise source (loudspeaker)	(700,150,200)
2	Reference microphone	(600,150,200)
3	Loudspeaker No. 1	(300,100,50)
4	Error microphone No. 1	(300,100,100)
5	Loudspeaker No. 2	(100,150,0)
6	Error microphone No. 2	(100,150,100)

ISBN: 978-988-19251-5-2
ISSN: 2078-0958 (Print); ISSN: 2078-0966 (Online)

TABLE IV
SOUND ATTENUATION IN 420 HZ SINE INPUT.

	Attenuation in channel 1	Attenuation in channel 2	Algorithm
Input Freq. 420 Hz	25	24	FXLMS
	29	27	EFNN

TABLE V
SOUND ATTENUATION IN 90 HZ SINE INPUT.

	Attenuation in channel 1			Attenuation in channel 2			Algorithm
Harmonic order	1^{st}	2^{nd}	3^{rd}	1^{st}	2^{nd}	3^{rd}	
Input Freq.	7	0	-5	8	-11	0	FXLMS
90 Hz	52	31	15	45	26	27	EFNN

REFERENCES

[1] Kim S. M. and Brenna M. J., A Compact Matrix Formulation Using the Impedance and Mobility Approach for the Analysis of the Structural Acoustic Systems, *Journal of Sound and Vibration*, vol. 223, no. 1, pp. 97-113, 1999.

[2] Kim S. M. and Brenna M. J., A Comparative Study of Feedforward Cornel of Harmonic and Random Sound Transmission into an Acoustic Enclosure, *Journal of Sound and Vibration*, vol. 266, no. 3, pp. 549-571, 1999.

[3] Kim S. M. and Brenna M. J., Active control of Harmonic Sound Transmission into an Acoustic Enclosure Using Both Structural and Acoustic Actuators, *Journal of the Acoustical Society of America*, vol. 107, no. 5, pp. 2523-2534, 2000.

[4] Jorge P. Arenas, On the Vibration Analysis of Rectangular Clamped Plates Using the Virtual Work Principle, *Journal of Sound and Vibration*, vol. 266, pp. 912-918, 2003.

[5] Jiu Hui Wu A.Q. Liu, H.L. Chen, Exact Solutions for Free-Vibration Analysis of Rectangular Plates Using Bessel Functions, ASME, *Journal of Applied Mechanics*, Vol. 74, pp. 1247-1251, 2007.

[6] Ravaud R., Lemarquand G., Roussel T., Time-varying Nonlinear Modeling of Electrodynamic Loudspeakers, *Applied Acoustics*, vol. 70, pp. 450-458, 2009.

[7] Kuo, S.M. and Morgan, D.R., "Active Noise Control Systems: Algorithms and DSP Implementation", *John Wiley & Sons Inc* , New York, 1996.

[8] Carmona J. C., Alvarado M., Active Noise Control of a Duct Using Robust Control, *IEEE Trans. On Control Systems Technology*, Vol. 8, No. 6, pp. 930-938, 2006.

[9] Qizhi Z., Yonglr J., Active Noise Hybrid Feedforward/Feedback Control Using Neural Network Compensation, *Transactions of the ASME*, Vol. 124, pp. 100-105, 2002.

[10] Zhang Q., Gan W., Zhou Y., Adaptive Recurrent Fuzzy Neural Networks for Active Noise Control, *Journal of Sound and Vibration*, vol. 296, pp. 935-948, 2006.

[11] Chen K.T., Chou C.H., Chang S.H. Liu Y.H., Adaptive Fuzzy Neural Network Control on the Acoustic Field in a Duct, *Applied Acoustics*, vol. 69, pp. 558-565, 2008.

[12] Sepehr S.R. and Ohadi A.R., Adaptive Fuzzy Neural Network Control on the Acoustic Field in a 3-D Enclosure with Flexible Panel, 16^{th} *International Conf. on Sound and Vib.*, pp. 1-8, 2009.

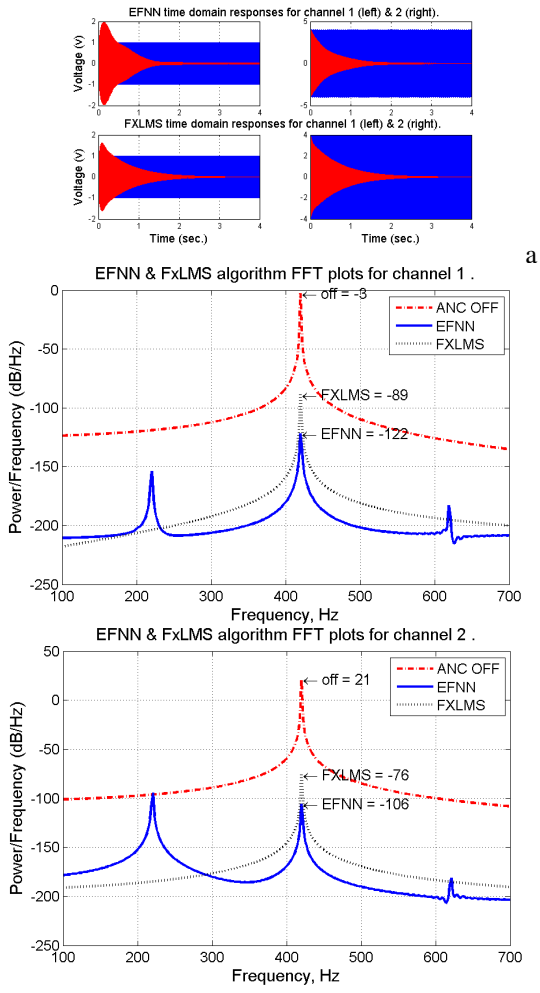

Fig. 6. Active 2 channel Enhanced FNN Noise Control in the enclosure with 420Hz sine input, time domain response (a) and Fast Fourier Transform FFT plot in channel 1 (b) & in channel 2 (c).

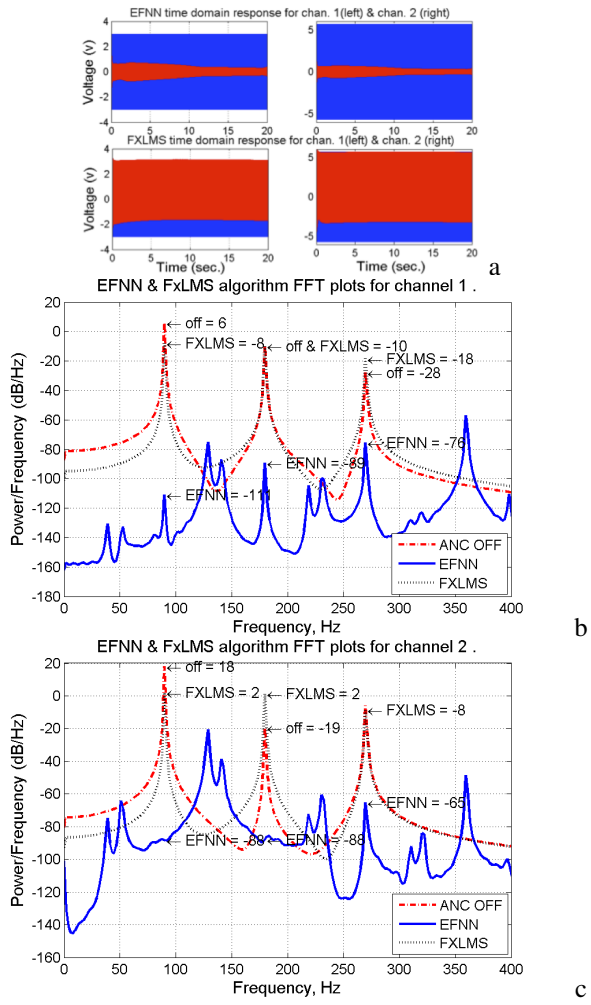

Fig. 7. Active 2 channel Enhanced FNN Noise Control in the enclosure with 90Hz sine input, time domain response (a) and Fast Fourier Transform FFT plot in channel 1 (b) & in channel 2 (c).

ISBN: 978-988-19251-5-2
ISSN: 2078-0958 (Print); ISSN: 2078-0966 (Online)